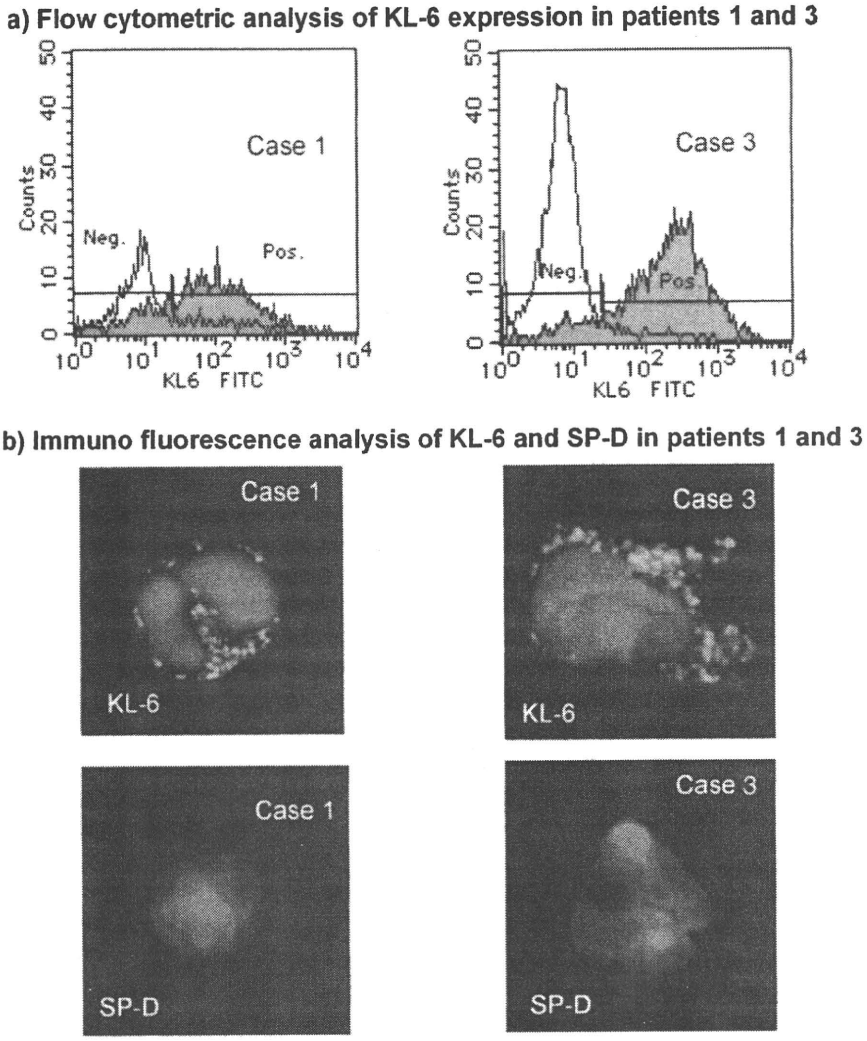

Fig. 4. Subcellular expression of KL-6 and SP-D in ATL cells. The subcellular expression of KL-6 and SP-D was examined by flow cytometry (a) and indirect immunostaining using anti-SP-D and anti-KL-6 antibodies (b). (a) Flow cytometric analysis revealed positive histograms (green) for KL-6, but negative for SP-D (neg., white) in ATL cells of patients 1 and 3. These patient numbers are consistent with Table 1. (b) Immunofluorescence staining showed positive signals (green) only for KL-6, and not for SP-D, in a smear of cells with multi-lobulated nuclei. The blue stains are nuclei labeled with DAPI.

patients had the elevated level of either KL-6 or SP-D, as shown in Table 1. Both markers were elevated in 2 patients (numbers 1 and 2). KL-6 was exclusively elevated in 6 patients (numbers 3 to 8), and SP-D was exclusively elevated in 7 patients (numbers 9 to 15). Interestingly, there was a substantial difference depending on the type of pulmonary complications observed in the groups exclusively expressing KL-6 or Sp-D (Table 1). Thus, the KL-6-expressing group was characterized by a predominance of lymphoma subtype (4 patients), leukemic cell invasion into the lungs (patients 2 and 4), demonstrated by cytology using bronchialveolar lavage fluid (BALF) or clinically suspected due to a reticular shadow on chest X-p (numbers 5, 6, and 7). In contrast, patients with a high serum level of only SP-D had pulmonary infectious complications but no leukemia-related pulmonary lesions.

To better understand the origin of serum KL-6 and SP-D, their subcellular expression was examined in ATL cells from 20 patients by flow cytometry and indirect immunostaining. KL-6 was detected with variable intensity on the cell surface as well as in the cytoplasm in 10 of the 20 ATL patients tested, whereas SP-D was not detectable in any patients. In particular, ATL cells obtained from patients 1 and 3 abundantly expressed KL-6, but not SP-D (Fig. 4 a and b). Hyperplasia of type II pneumocytes was histologically observed in a patient with ATL with pulmonary leukemic invasion (Fig. 5). All of these data suggest that KL-6 in the serum is partially derived from these pneumocytes or from the ATL cells themselves.

We then compared KL-6 and SP-D serum levels with LD activity and sIL-2R levels that are well-characterized biomarkers. sIL-2R is a good surrogate marker for the evaluation of malignant behavior and tumor burden in ATL. There was neither a statistically significant correlation

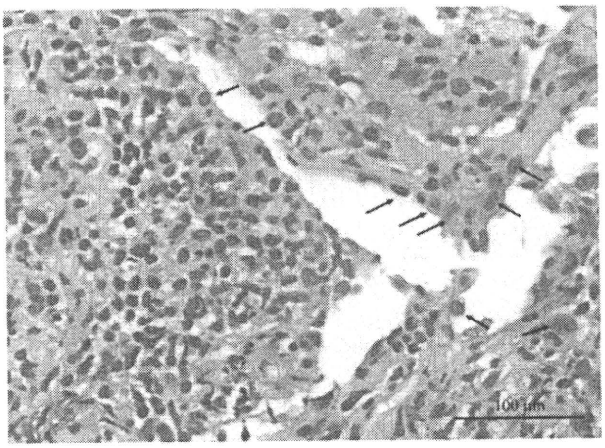

Fig. 5. Histological examination of a lung sample with ATL cell invasion. Hyperplasia (arrow head) of type II pneumocytes was observed with massive invasion of CD4-positive ATL cells (Patient No.4 in Table1). Hyperplasia of type II pneumocytes indicated pulmonary leukemic invasion of ATL cells.

between KL-6 and LD ($r = -0.012$, $p = 0.959$), nor between KL-6 and sIL-2R ($r = 0.0126$, $p = 0.919$), suggesting that the clinical significance of KL-6 is independent of the pathology represented by LD or sIL-2R. In contrast, SP-D had a tendency to correlate with LD but not with sIL-2R, further suggesting that the clinical significance of KL-6 and SP-D differs.

Discussion

We present the data that show an elevation of serum KL-6 and SP-D levels in about 10% of patients with hematological malignancies. Interestingly, the elevation of these markers was mutually exclusive. There was no noticeable difference in the incidence of the elevated serum KL-6 and SP-D among disease subtypes of ALL, AML, CML, CLL, ML, and ATL. The only reports we found in the literature were several case reports showing that serum KL-6 happened to be elevated when cytomegalovirus or pneumocystis jiveroci pneumonia was present as a complication during intensive chemotherapy in patients with ALL (Takahashi et al. 2001), ML and ATL (Tanaka et al. 2002). More interestingly, Fujisawa et al. (2007) reported a case of peripheral T cell lymphoma (PTCL) with elevated serum KL-6 derived from reactive proliferative pneumocytes due to pulmonary invasion of tumor cells. These data indicate that soluble KL-6 in the serum is associated with pulmonary complications of infective interstitial pneumonia rather than hematological malignancies. However, our data presented here differ from these previous reports in that patients with high serum levels of KL-6 showed a trend of leukemic infiltration into the lung, but no overt infectious pulmonary complications, as shown for the ATL patients in Table 1. On the other hand, SP-D may be a useful marker of the presence of infectious lung diseases that occur as a complication in patients with ATL. Indeed, none of 7 patients that showed exclusive elevation of SP-D had leukemic cell invasion into the lung, but all of these patients did have complications with infectious pulmonary disorders. All of these findings suggest that measurement of the combined levels of serum KL-6 and SP-D represents a possible method to discriminate leukemic invasion from infectious pulmonary complications, at least in ATL. At present, there are difficulties in the invasive collection of BALF for differential diagnosis of leukemic invasion or interstitial pneumonias, which are frequent complications in ATL. Therefore, KL-6 and SP-D are promising markers for such differential diagnosis, because the assay methods are simple and are measured without invasion.

Currently, the origin of serum KL-6 in cancer patients is controversial. Although there are reports that cancer cells themselves produce KL-6 (Kohno et al. 1992), our data indicate that ATL cells probably also express KL-6, suggesting that serum KL-6 originates from ATL cells. However, elevated serum KL-6 in ATL was observed only in patients with pulmonary leukemic cell invasion, but not in ATL patients without this complication. In addition, hyperplasia of type II pneumocytes was histologically observed in an ATL patient with leukemic lung invasion. These findings suggest that a biological relationship exists between pneumocytes and ATL cells via KL-6 with regard to lung invasion and cell-growth at invasive sites. That is, aberrant overexpression of KL-6 may account in part for the lung invasion of ATL cells, because KL-6 has been recently shown to be involved in cell-cell co-adhesive infiltration and proliferation (Teruya-Feldstein et al. 2003).

In conclusion, although serum KL-6 and SP-D are rarely elevated in patients with hematological malignancies including ATL, the elevation of either KL-6 or SP-D can be used as a marker to discriminate leukemic invasion from infectious pulmonary complications.

References

Brossart, P., Schneider, A., Dill, P., Schammann, T., Grunebach, F., Wirths, S., Kanz, L., Bühring, H.J. & Brugger, W. (2001) The epithelial tumor antigen MUC1 is expressed in hematological malignancies and is recognizaed by MUC1-specific cytotoxic T-lymphocytes. *Cancer Res.*, **61**, 6846-6850.

Fujisawa, T., Suda, T., Matsuura, S., Enomoto, N., Takeshita, K., Ohnishi, K. & Chida, K. (2007) Peripheral T-cell lymphoma with diffuse pulmonary infiltration and an increase in serum KL-6 level. *Respirology*, **12**, 452-454.

Kamihira, S., Atogami, S., Sohda, H., Momita, S., Yamada, Y. & Tomonaga, M. (1994) Significance of soluble interleukin-2 receptor levels for evaluation of the progression of adult T-cell leukemia. *Cancer*, **73**, 2753-2758.

Kohno, N. (1999) Serum marker KL-6/MUC1 for the diagnosis and management of interstitial pneumonitis. *J. Med. Invest*, **46**, 151-158.

Kohno, N., Akiyama, M., Kyoizumi, S., Hakoda, M., Kobuke, K. & Yamakido, M. (1988) Detection of soluble tumor-associated antigens in sera and effusions using novel monoclonal antibodies, KL-3 and KL-6, against lung adenocarcinoma. *Jpn. J. Clin. Oncol.*, **18**, 203-216.

Kohno, N., Hamada, H., Fujioka, S., Hiwada, K., Yamakido, M. & Akiyama, N. (1992) Circulating antigen KL-6 and lactate

dehydrogenase for monitoring irradiated patients with lung cancer. *Chest*, **102**, 117-122.

Leth-Larsen, R., Nordenbaek, C., Tornoe, I., Moller, V., Schlosser, A., Koch, C., Teisner, B., Junker, P. & Holmskov, U. (2003) SP-D serum levels in patients with community-acquired small star, filled. *Clin. Immunol.*, **108**, 29-37.

Marcaurelle, L.A. & Bertozzi, C.R. (2002) Recent advances in the chemical synthesis of mucin-like glycoproteins. *Glycobiology*, **12**, 69R-77R.

Mukherjee, P., Tinder, T.L., Basu, G.D. & Gendler, S.J. (2005) MUC1(CD227) interacts with lck tyrosine kinase in Jurkat lymphoma cells and normal T cells. *J. Leukoc. Biol.*, **77**, 90-99.

Shimoyama, M. (1991) Diagnostic criteria and classification of clinical subtypes of adult T-cell leukaemia-lymphoma. A report from the Lymphoma Study Group (1984-87). *Br. J. Haematol.*, **79**, 428-437.

Stahel, R.A., Gilks, W.R., Lehmann, H.P. & Schenker, T. (1994) Third international workshop on Lung Tumor and differentiation antigens: overview of the results of the central data analysis. *Int. J. Cancer*, **Suppl, 8**, 6-26.

Takahashi, T., Ebihara, Y., Manabe, A., Tsuji, K., Nakamura, T., Nakahata, T. & Iwamoto, A. (2001) SP-D and KL-6 as a serologic indicators of *pneumocystis carinii* pneumonia in a child with acute lymphoblastic leukemia. *J. Med.*, **32**, 41-51.

Tanaka, M., Tanaka, K., Fukahori, S., Fujimatsu, Y., Jojima, H., Shiraishi, K., Honda, J. & Oizumi, K. (2002) Elevation of serum KL-6 levels in patients with hematological malignancies associated with cytomegalovirus or *Pneumocysis carinii* pneumonia. *Hematology*, **7**, 105-108.

Teruya-Feldstein, J., Donnelly, G.B., Goy, A., Hegde, A., Nanjangud, G., Qin, J., Thaler, H., Gilles, F., Dyomin, V.G., Lloyd, K.O., Zelenetz, A.D., Houldsworth, J. & Chaganti, R.S. (2003) MUC-1 mucin protein expression in B-cell lymphomas. *Appl. Immunohistochem. Mol. Morphol.*, **11**, 28-32.

White, J.D., Zaknoen, S.L., Kasten-Sportes, C., Top, L.E., Navarro-Roman, L., Nelson, D.L. & Waldmann, T.A. (1995) Infectious complications and immunodeficiency in patients with human T-cell lymphotropic virus I-associated adult T-cell leukemia/lymphoma. *Cancer*, **75**, 1598-1607.

European Journal of Haematology ISSN 0902-4441

ORIGINAL ARTICLE

Aberrant p53 protein expression and function in a panel of hematopoietic cell lines with different p53 mutations

Shimeru Kamihira[1], Chiharu Terada[1], Daisuke Sasaki[1], Katsunori Yanagihara[1], Kunihiro Tsukasaki[2], Hiroo Hasegawa[1], Yasuaki Yamada[1]

Departments of [1]Laboratory Medicine and [2]Hematology, Nagasaki University Graduate School of Biomedical Sciences, Nagasaki, Japan

Abstract

The *p53* gene is one of the most important genes involved in carcinogenesis and its role in part has been clarified by research using cell lines. To know the comprehensive characteristics of 22 hematopoietic cell lines (T, 13 and non-T, nine lines), the relationship between p53 mutational status, its altered functioning, and its mRNA and protein levels were examined. p53 mutations were less frequent in T-cell lines (38% vs. 78%) with mainly single nucleotide substitutions generating missense codons. Of 22 different p53 mutations, 12 (54.5%) resulted in mutated proteins, with the mutations clustering mainly in the sequence-specific DNA-binding site region located from amino acid residues 102 to 292. *p53* mRNA and protein assays determined that wild-type cell lines expressed constant levels of both mRNA and protein, but mutated cell lines demonstrated two expression patterns: protein over-expression with reduced mRNA levels, because of missense mutations; and protein under-expression with little mRNA expression, because of other mutations. The resistance to Nutlin (MDM2 inhibitor)-induced apoptosis was associated with p53 mutations independently of MDM2 expression levels. This clarification of the unique associations in cell lines useful for bio-medical studies will contribute to a better understanding of p53-associated carcinogenesis.

Key words p53; mutation; haplo-insufficiency; hematologic cell line; adult T-cell leukemia

Correspondence Shimeru Kamihira, PhD, MD, Department of Laboratory Medicine, Nagasaki University Graduate School of Biomedical Sciences, 1-7-1, Sakamoto, Nagasaki 852-8501, Japan. Tel: +81 95 819 7407; Fax: +81 95 819 7422; e-mail: kamihira@nagasaki-u.ac.jp

Accepted for publication 22 December 2008

doi:10.1111/j.1600-0609.2009.01211.x

The tumor suppressor gene *p53* is located on the short arm of chromosome 17 and plays a central role in control of the cell cycle, DNA repair, and activation of apoptosis. Abrogation of these *p53* functions is thought to be involved in carcinogenesis (1, 2). *p53* knockout mice have an increased tendency to develop spontaneous tumors. It was previously thought that transformation required the inactivation of both *p53* alleles, i.e., loss of heterozygosity, but recent studies have shown that *p53* function can also be disrupted by haplo-insufficiency; i.e., the alteration of one allele of the gene with the other allele remaining normal (3). Inactivation of the *p53* gene is known to be caused by genetic and epigenetic mechanisms, such as mutation, methylation, and interaction with viral proteins. *p53* alterations are widely observed in at least 50% of human tumors, including hematologic malignancies, with colon, breast, and lung cancers having the highest frequencies of *p53* mutations (2, 4).

Mutant p53 proteins encoded by mutated alleles have several characteristics that differ from those of wild-type p53, including a longer half-life and a dominant negative effect on wild-type p53. Furthermore, the dominant negative function seems to vary according to the polymorphic status of codon 72 (C466G; arginine vs. proline) (5). These characteristics of the mutant protein appear to account for its over-expression in tumor cells harboring the mutated gene, and which demonstrate biologically aggressive behavior and chemoresistance (6–8). The presence of *p53* mutations and over-expression of p53 protein has a strong prognostic impact (9, 10). Several studies

have reported that adult T-cell leukemia (ATL) patients demonstrate mutational inactivation of p53 in 20–40% of cases, and that gene inactivation contributes to the development of malignant phenotypes (11).

The Nutlins, *cis*-imidazoline analogs, are novel small-molecule inhibitors of MDM2, which bind to MDM2, releasing them from negative control by the p53 pathway and leading to effective p53 stabilization and activation in wild-type cells (12). However, little is known about the association between *p53* mutational status and expression levels and functioning of p53 protein. Accordingly, using a panel of hematopoietic cell lines available as bio-source to study oncology, we examined the associations between *p53* mutations, p53 functional status, and mRNA and protein levels.

Materials and methods

Cell lines

The hematopoietic cell lines used included six ATL-derived T-cell lines, three human T-cell leukemia virus type-1 (HTLV-1)-infected T-cell lines, four T-cell lines without HTLV-1, five lymphoma-derived B-cell lines, two monocytic cell lines, and two others. All but three (MT1, MT2, and HUT102) of the ATL cell lines were established in our laboratory (13). The other cell lines were obtained from the American Type Culture Collection (Rockville, MD, USA), and the Hayashibara Bio Inc (Okayama, Japan). Each cell line was cultured according to the supplier's, or our, protocols.

High molecular weight DNA was extracted from cell lines using a QIAmp DNA Blood Mini kit (Qiagen GmbH, Hilden, Germany). Total RNA was extracted using ISOGEN (Nippon Gene, Toyama, Japan). After removing contaminating genomic DNA using a Message Clean kit, cDNA was synthesized using Oligo (dT) 12–18 Primer and SuperScript III Reverse Transcriptase (Invitrogen Corp., Carlsbad, CA, USA). All primers and probes used in this study were designed using Primer3Plus (14) (The sequences of all primers and probes used here are available via an e-mail of kamihira@nagasaki-u.ac.jp).

Mutational analysis

A 1376-bp fragment including the *p53* mRNA open reading frame (ORF) was amplified by polymerase chain reaction (PCR) using primers S1 and AS1. The standard thermal cycling conditions were an initial 98°C for 30 s followed by 35 cycles at 98°C for 10 s and 67°C for 1 min. The amplicons were subjected to direct sequencing analysis to identify mutations in the *p53* ORF. The PCR primers used for cycle sequencing were S1, S2, and S3 for anti-sense products, and AS1, AS2, and AS3 for sense products. Cycle sequencing was performed using a BigDye Terminator v3.1 Cycle Sequencing Kit (Applied Biosystems, Foster City, CA, USA) and an Automated DNA Sequence Analyzer (Model 3100; Applied Biosystems, Foster City, CA, USA). Sequence data for the *p53* ORF region were compared with the published *p53* mRNA sequence (NM_00546).

Real time RT-PCR quantification for *p53* and *mdm2* mRNA levels

Primers and TaqMan probes labeled with TAMRA dye at the 3′ end and FAM at the 5′ end were designed. The mRNA levels for *p53*, *mdm2*, and porphobilinogen deaminase (*PBGD*) were measured from a cDNA template using a LightCycler480 PCR System (Roche Diagnostics, Mannheim, Germany). Briefly, reactions were performed in a 20 μL volume with 5 μL 1/10 diluted cDNA, 0.5 μM PCR primers, 0.1 μM TaqMan probes, and 10 μL of 20 LightCycler 480 probes (Master Mix; Roche Diagnostics). The PCR program consisted of 95°C for 5 min followed by 50 cycles of 95°C for 10 s and 60°C for 30 s. After 50 cycles, the absolute amounts of *p53*, *mdm2*, and *PBGD* mRNA were interpolated from the standard curves generated by the dilution method using plasmids derived from a clone transfected with pTAC-1 Vector (BioDynamics Laboratory Inc., Tokyo, Japan) containing amplicons from the *p53*, *mdm2*, and *PBGD* genes, respectively. To normalize these results for variability in concentration and integrity of RNA and cDNA, the *PBGD* gene was used as an internal control in each sample.

Measurement of p53 protein

Total p53 protein in cell lysates (10 μg) was measured using the Luminex$^{100™}$ System (Hitachi Software Engineering Co., Tokyo, Japan), and the total p53 Antibody Bead Kit (LHO0151, Biosource International, Camarillo, CA, USA), according to the manufacturers' instructions. In brief, cells were washed three times with phosphate-buffered saline and pelleted cells were homogenized at 4°C in lysis buffer (0.1% sodium dodecyl sulfate, 1% Igepal CA-630, and 0.5% sodium deoxycholate) and a protease inhibitor cocktail (Sigma, St Louis, MO, USA). Sample solutions appropriately diluted with assay diluent were incubated with anti-p53 antibody-coupled beads for 2 h at room temperature on an orbital plate shaker, washed three times with wash solution, and the beads were further incubated with biotinylated detector antibody for 1 h. This was followed by incubation with streptavidin–R-phycoerythrin for 30 min at room temperature, and washing, after which the suspended beads were analyzed using the Luminex$^{100™}$ System. A

standard curve was created using serially diluted recombinant p53, and the p53 concentrations in samples were estimated.

Assays for p53 activation

The degree of DNA-binding capacity and the phosphorylation at serine 15 ($p53^{ser15}$) were analyzed as markers of p53 activation, using a TransAM™ p53 Transcription Factor Assay kit (Active Motif, Carlsbad, CA, USA) and an anti-phospho-$p53^{ser15}$/total p53 Multiplex Bead-based system (BioSource International) available for Luminex technology. The degree of activation was demonstrated by the fold induction of the DNA-binding capacity of p53 and the fold induction of phosphorylation of $p53^{ser15}$, relative to the measures before and after treatment with Nutlin-3.

Briefly, nuclear extracts from cells treated with 10 μM Nutlin-3 (Sigma Aldrich, St Louis, MO, USA) for 24 h were diluted in 10 μg of total protein with lysis buffer and applied to plates with immobilized oligonucleotides containing the p53 consensus binding site. After 1 h at room temperature, plates were washed and incubated with p53 antibody, followed by secondary antibody and developing solution. Color generated as a marker of the DNA-binding capacity was read at 450 nm. The procedure was performed according to instructions for the TransAM™ p53 and the Luminex$^{100™}$.

The phosphorylation of $p53^{ser15}$ was analyzed using anti-p53 and anti-phospho $p53^{ser15}$ according to the Luminex$^{100™}$ system protocol, as described above. The final outcome of p53 activation was determined by the degree of apoptosis induced by Nutlin-3 using the annexin V/propidium iodide double staining flow-cytometric method (15).

Statistical analysis

The chi-squared and Fisher's exact tests were used to examine categorical data, and the Mann–Whitney *U*-test

Table 1 Characteristics of cell lines tested and summary of *p53* mutations and deduced amino acid sequences

Cell line	Origin	RT-PCR products	Event				p53 status
			Exon	Codon	Sequence	aa	
SO4	ATL cell	1.4 kb (Arg)[2]	6	223	C919A	Missense (Pro → His)	Mt
ST1	ATL cell	1.4 kb (Pro)					Wt
KK1	ATL cell	1.4 kb (Pro)	3	31	G342A	Missense (Val → Ire)	Mt
			5	152	C706T)	Missense (Pro → Arg)	
KOB	ATL cell	1.4 kb (Pro)					Wt
LM-Y1	ATL cell	1.4 kb (Arg)	4	36	G359A	Silent	Wt
MT1	ATL cell	1.4 kb (Arg)	5	176	G778A	Missense (Cyt → Tyr)	Mt
OMT	HTLV-1 infected T	1.4 kb (Pro)					Wt
MT2	HTLV-1 infected T	1.4 kb (Arg)					Wt
HUT102	HTLV-1 infected T	1.4 kb (Arg)					Wt
MT1s	Non-HTLV-1 T	1.4 kb (Arg)	5	149	C697T	Missense (Ser → Phe)	Mt
MT1g	Non-HTLV-1 T	1.4 kb (Arg)					Wt
MOLT4	Non-HTLV-1 T	1.4 kb (Arg)					Wt
Jurkat	Non-HTLV-1 T	1.4 kb (Arg)	5	125	G626A	Missense (Thr → Arg)	Mt
			6	196	C837T	Nonsense (Stop)	
		1.2 kb (del)	4	59–125	425–625	Deletion 199[1]	
			10	360	1329(G)	Deletion 1[1]	
SuDHL	B-cell lymphoma	1.4 kb (Arg)					Wt
Ramos	B-cell lymphoma	1.4 kb (Arg)	7	254	A/T1011/2G/A	Missense (Ile → Asp)	Mt
SKW6.4	B-cell lymphoma	1.4 kb (Arg)					
		1.2 kb (Pro)	4	59–125	426-624	Deletion 199[1]	Mt
HS-sultan	Myeloma	1.4 kb (Pro)					Wt
CA46	Burkitt lymphoma	1.4 kb (Pro)	7	248	G994A	Missense	Mt
THP1	Monocytic leukemia	1.4 kb (Arg)	5	174–182	770–795	Deletion 25[1]	Mt
U937	Monocytic leukemia	1.4 kb (Arg)	4	105	G564A	Missense (Gly → Ser)	Mt
			5	125	G626A	Silent	
			6	196	C837T	Nonsense (stop)	
		1.2 kb (del)	4	59–125	425–625	Deletion 199[1]	
HL60	Myeloid leukemia	No-detected				Deletion	Mt
K562	Erythroblastic leukemia	1.4 kb (Pro)	5	135	655(C)	Insertion[1]	Mt

[1]Frame shift (stop codon).

[2]p53 codon 72 polymorphic status, C466G.

and Kruskal–Wallis tests were used for non-parametric data. Differences in the strength of the association between two variables were evaluated by the Spearman's rank correlation coefficients. Differences were considered statistically significant when *P*-values were <0.05.

Results

Mutation profiles of cell lines

Using the present RT-PCR protocol, two main, distinct products of about 1.4 and 1.2 kb were generated in Jurkat, U937, THP1, K562, and SKW6.4 cells, while the remaining 16 cell lines, excluding HL-60 cells, showed a single band of 1.4 kb. No amplified products were observed in HL-60 cells. The results from direct sequencing of the amplicons are summarized in Table 1. Overall, 20 *p53* mutations were identified in 13 of 22 cell lines (59.0%). The mutations were located in exons 3 (one event), 4 (five events), 5 (seven events), 6 (two events), 7 (two events), and elsewhere (two events). Clustering was observed in exons 4 and 6, which is a highly conserved region including the sequence specific DNA-binding sites from amino acids 102 to 292. Of the 20 mutations, 13 (65%) were single nucleotide substitutions, whereas six (30%) were found to be deletions or insertions with frame-shifts generating stop codons. The 13 single nucleotide substitutions consisted of nine missense (69.2%), two nonsense, and two silent mutations. Missense mutations were mainly detected in T-cell lines, whereas deletions and nonsense mutations were mainly detected in B-cell and myeloid cell lines. Fifteen of the 22 mutations, such as C919C, C706T, G342A, G359A, G778A, G778A, C697T, G626A, C626A, C837T, AT1011GA, G994A, 174-182del, G564A, and 655(ins C), were accordant with the previous reports (IARC TP Mutation Database and The TP53 Web site). On the other hand, four kinds of the mutations detected in Jurkat, SKW6.4 and U937 have not yet reported. In particular, 199 base pair deletion (nt 425–625) in exon 4 was detected in only the 1.2 kb PCR products, suggesting that it is derived from a splicing form. Consequently, five of 13 T-cell lines and seven of nine non-T-cell lines (totally 12/22, 54.5%) were deduced to carry mutant p53 proteins. Regarding the relationship between mutations and the genotype of the p53 codon 72 polymorphism (arginine vs. proline), mutations were demonstrated to be in arginine-encoding alleles in nine cell lines, and in proline-encoding alleles in three cell lines, indicating that mutations occurred more frequently in the arginine-encoding alleles (69.2% vs. 23.10%, $P = 0.04$), as shown in Tables 1 and 2.

Association of *p53* mutational status with its mRNA and protein levels

The *p53* mRNA levels differed significantly between the wild-type and the mutated cell lines (0.62 vs. 0.37 $P = 0.048$). The p53 protein levels varied widely from 0 to 15 000 pg/mL, but the mean values were not significantly different between the wild-type and the mutated cell lines (4160 vs. 3860 pg/mL). The p53 protein levels in all cell lines failed to correlate with the p53 mRNA levels, although specific cell lines with protein levels of <1000 pg/mL showed tendencies toward inverse correlations between *p53* mRNA and protein levels ($r = -0.4636$, the Spearman *U*-test), as shown in Fig. 1. Furthermore, Fig. 1 shows the distinctive distribution of the cell lines which formed three clusters, designated as A, B, and C. Wild-type cell lines clustered in the center area (A), representing balanced expressions of p53

Table 2 Comparison of *p53* codon 72 (C466G) polymorphic status in wild-type and mutated groups

		p53 codon 72 (C466G) status		
p53 mutation	*n* (%)	Arg (%)	Pro (%)	*Unknown (%)*[1]
Wild-type	9 (41.0)	5 (55.5)	4 (45.5)	*0*
Mutated	13 (59.0)	9 (69.2)*	3 (23.1)**	*1 (7.7)*
Total	22 (100)	14	7	*1*

The allelic frequency was dominant for the arginine-encoding allele compared to the proline-encoding allele (* vs. **; $P = 0.0405$).
[1]Unknown due to complete deletion.

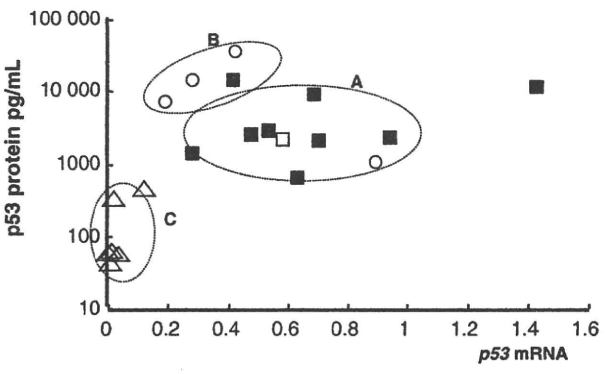

Figure 1 Twin dot graph of p53 protein (*Y*-axis) and mRNA (*X*-axis) expression levels in cell lines categorized according to their *p53* mutational status. Solid square; wild-type, open circle; missense, open triangle; other mutations, gray square; silent mutation. No correlation between *p53* mRNA and protein levels ($r = 0.238$, $P = 0.175$). However, a unique association among the types of mutations, *p53* mRNA and protein was observed, because solid squares are clustered into the central area (A), while mutated cells are separated into two clusters of B and C: The cell lines with wild-type sequences had balanced levels of transcripts and proteins, and cell lines with mutants were subdivided into two groups, with either over-expressed or under-expressed protein levels, with low mRNA expression.

mRNA and protein. Mutated cell lines clustered into two areas, B and C; missense mutated cell lines fell into cluster B, and cell lines with mutations other than missense mutations (non-missense mutated cells) fell into cluster C. Thus, mutated cells were subdivided into two groups characterized by different imbalances in expression patterns between the transcript and protein levels because of mutations.

The *mdm2* mRNA levels also failed to correlate with either the *p53* mRNA ($r = 0.256$, $P = 0.152$) or protein ($r = 0.1059$, $P = 0.409$) levels. Differences in expression levels between wild-type and mutated cell lines were found only for *p53* mRNA, but not for p53 protein or *mdm2* mRNA. However, among the three groups of wild-type, missense mutated, and non-missense mutated cell lines, the association with *p53* mutational status was the highest for p53 protein levels, followed by *p53* mRNA levels, and then *mdm2* mRNA levels ($P = 0.0033$ vs. 0.0042 vs. 0.081, Kruskal–Wallis test).

Table 3 Comparison of total p53 protein concentration and the degree of p53 activation induced by Nutlin-3 in the various cell lines

		Nutlin-Induced p53 activation		
	p53 protein (ng/ml)[1]	DNA-binding capacity (induction fold)[2]	Phospho-p53^{ser15} (induction fold)[2]	Apoptosis (degree)[3]
Wild-type cells				
ST1	1.59	15.0	16.3	++
KOB	5.47	2.5	4.2	+
LM-Y1	3.82	3.9	6.1	+
OMT	5.85	2.8	19.8	+
MT2	2.58	3.5	8.9	+
HUt102	2.21	4.5	20.9	+
MOLt4	1.65	14.7	19.6	+
SuDHL	3.92	5.1	12.5	++
HS-Sultan	8.65	nt	nt	–
Mutant cells with missense				
KK1	5.23	2.2	0.8	+/–
Ramos	10.17	1.4	1.2	–
MT1s	1.17	10.7	11.8	+
SO4	15.00	2.4	1.5	–
Mutant cells without missense				
Jurkat	0.44	<0.1	<0.5	–
THP1	0.06	NC	NC	–
U937	0.26	NC	NC	–
HL60	0.07	NC	NC	–
K562	0.07	NC	NC	–

NC, no change in fold induction.

[1]The p53 protein concentration was displayed as pg/10 μg cell lysates.

[2]The degree of the DNA-binding and phospho-p53^{ser15} capacity was scored as induction fold relative to the measures before and after treatment with Nutlin-3.

[3]Apoptotic cells assessed as cells staining for annexin-V and propidium iodide (++, 50% or more; +, 10–50%; ±, 10% or less).

Analysis of p53 activation induced by Nutlin-3

To analyze, the activation of p53 aberrantly expressed in the cell lines, a transcription factor assay was performed as a marker of the DNA-binding capacity and the phosphorylation assay was performed to detect p53^{ser15}. These assays showed characteristic results specific for each group, classified according to the type of mutations, as summarized in Table 3. In wild-type cell lines, p53 was expressed at intermediate levels, and the DNA-binding and phosphorylation capacity of p53 were evident, leading to apoptosis after treatment with Nutlin-3. However, although missense mutated cell lines expressed high levels of p53 protein, the DNA-binding and phosphorylation capacities were poor and apoptotic induction varied, indicating that the quantity and function of missense mutated p53 were not associated. In non-missense mutated cell lines, p53 protein was rarely detected, and p53 activation and apoptosis were not induced.

Discussion

p53 mutations currently have the distinction of being the commonest mutations found in human cancers, including hematologic malignancies. *p53* is a tumor suppressor gene and inactivation of *p53* function is a causative event in oncogenesis.

This study analyzed *p53* mutational status in the entire ORF, and the types of mutations were related to the quantitative expression of *p53* mRNA and protein in 22 hematopoietic cell lines. The results showed that half of the cell lines harbored *p53* mutations and that the mutations occurred preferentially in arginine-encoding alleles of the *p53* codon 72 polymorphism. Notably, four of nine ATL-derived cell lines had carried p53 mutations on different sites with three missense and one silent. The p53 protein levels in mutated cells were not correlated with the levels of *p53* mRNA, and cells with missense mutations exclusively harbored over-expressed p53 proteins. Mutated p53 proteins, despite of over-expression, were defective for Nutlin-mediated activation and stabilization. These abnormalities in both the levels and functioning of the p53 protein depended on the type of mutations, and not solely on the presence of mutations.

The frequency of *p53* mutations found in these cell lines seems to be slightly higher than, or similar to, that found in primary hematologic malignancies, such as 39% in acute lymphoblastic leukemia, 44% in ATL, 32% in acute myelogenous leukemia, and 42% in chronic lymphocytic leukemia (16–18). Most mutations detected in this study were single nucleotide substitutions, being

mainly missense mutations, followed by deletion, insertion, nonsense, and silent mutations. About 90% of the mutations were located from amino acids 102 to 292, which contains the DNA-binding domain. Consistent with results on the *p53* codon 72 polymorphism involving in the dominant-negative function and cancer risk (19, 20), *p53* mutations found in cell lines in this study occurred preferentially in the arginine-encoding alleles. In contrast, the allelic frequency in the wild-type cell lines was almost the same as in Japanese controls; 0.55 (Arg) vs. 0.45 (Pro) in this study, and 0.58 and 0.42 in Japanese controls. These *p53* mutational profiles of hematologic cell lines are similar to the pattern found in primary malignant solid tumors and hematologic malignancies reported in the database by Prokocimer *et al.* (18).

MDM2 mediates the ubiquitin-dependent degradation of p53, enhancing tumorigenic potential and resistance to apoptosis. Our data showed that the resistance to Nutlin-mediated apoptosis was basically associated with the presence and type of p53 mutations, although there existed several exceptional cases, such as HS-Sultan and MT1s (Table 3). This means that many complicated factors alternative to MDM2-p53 interaction, such as anti-apoptotic inhibitors, ATM, single polymorphic gene, and so on, may be involved in the Nutlin-induced apoptosis. A unique association between *p53* mutational status and *p53* mRNA and protein expression levels, quantified by real-time RT-PCR and Luminex methods, was also demonstrated in this study. The expression levels of *p53* mRNA in mutated cell lines were lower than in wild-type cell lines, indicating that *p53* mRNA quantification is useful for detecting the presence or absence of mutations. The present data on *p53* mRNA quantification were similar to those reported by Baumbush *et al.* (21), whose data showed that the expression levels of *p53* mRNA were highest in mutated tumors with missense mutations, followed by wild-type tumors, and then mutated tumors with nonsense and deletion mutations. Although the *p53* mRNA levels quantified by RT-PCR seem to show a marked variability, the aberrant expression of *p53* mRNA in mutated cell lines seemed to be consistent. Mutated cell lines with missense mutations over-expressed p53 protein despite having lower mRNA expression levels than in wild-type cell lines. Recent studies have shown that the p53 protein levels do not necessarily correlate with p53 mRNA at the transcript level, even in normal cells, because of the short half-life of the wild-type p53 protein (1). This study found that p53 over-expression was closely associated with missense mutations, but was not correlated with *p53* mRNA or *mdm2* mRNA expression levels. This finding suggests that structural alterations of the mutant protein modulated by missense mutations may be involved in the degradation of the protein, through post-translational modification (22–24). However, cell lines with non-missense mutations had neither detectable levels of *p53* mRNA nor protein. This is probably explained by impairment of the pretranslational stage. Overall, this unique association implies that *p53* mutations can affect the expression levels and functioning of the p53 protein.

In conclusion, the results of this study suggest that the frequency of *p53* mutations in hematopoietic cell lines is 50%. They also demonstrate that a unique association exists between the *p53* mutational status and the expression levels and functioning of its mRNA and protein, which depended not only on the presence or absence of mutations but also on the type of mutation. The characteristics observed in mutated cell lines could act as biomarkers to allow the better understanding of *p53*-associated tumor biology, and for screening for *p53* status in clinical settings.

Acknowledgements

This study was supported financially by a Japanese national grant, Kakenn, No. 17390165.

Author's contribution

SK designed this study, interpreted the data, and wrote the manuscript. AU, TT, DS, HH, and KY carried out molecular experiments, and KT and YY supplied and maintained cell lines and interpreted the data.

Competing interests

The authors declare that they have no competing interests.

References

1. Lain S, Lane DP. Tumor suppressor genes. In: Knowles M, Selby P, eds. *Introduction to the Cellular and Molecular Biology of Cancer*. Oxford: Oxford Press, 2005:135–55.
2. Poeta ML, Manola J, Goldwasser MA, *et al.* TP53 mutations and survivin in squamous-cell carcinoma of the head and neck. *N Eng J Med* 2007;**357**:2552–61.
3. Quon KC, Berns A. Haplo-insufficiency? Let me count the way. *Genes Dev* 2001;**2**:113–23.
4. Soussi T, Asselain B, Hamroun D, Kato S, Ishioka C, Claustres M, Beroud V. Meta-analysis of the *p53* mutation database for mutant *p53* biological activity reveals a methodological bias in mutation detection. *Clin Cancer Res* 2006;**12**:62–9.
5. Thomas M, Kalita A, Labrcque S, Pim D, Banks L, Matlashewski G. Two polymorphic variants of wild-type p53 differ biochemically and biologically. *Cell Mol Biol* 1999;**19**:1029–100.

6. Concin N, Zeillinger C, Tong D, *et al.* Comparison of *p53* mutational status with mRNA and protein expression in a panel of 24 human breast carcinoma cell lines. *Breast Cancer Res Treat* 2003;**79**:37–46.
7. Lynch LC, Milner J. Loss of one *p53* allele results in four-fold reduction of *p53* mRNA and protein: a basis for *p53* haplo-insufficiency. *Oncogene* 2006;**25**:3463–70.
8. Russo A, Migliavacca M, Zanna I, *et al. p53* Mutations in L3-loop zinc-binding domain, DNA-ploidy, and S phase fraction are independent prognosis indicators in colorectal cancer: a prospective study with a five-year follow-up. *Cancer Epidemiol Biomarkers Prev* 2002;**11**:1322–31.
9. Anensen N, Haaland I, D'Santos C, Van Belle W, Gjertsen BT. Proteomics of p53 in diagnostics and therapy of acute myeloid leukemia. *Curr Pharm Biotechnol* 2006;**7**:199–207.
10. Renneville A, Roumier C, Biggio V, Nibourel O, Boissel N, Fenaux P, Preudhomme C. Cooperating gene mutations in acute myeloid leukemia: a review of the literature. *Leukemia* 2008;**22**:915–31.
11. Tawara M, Hogerzeil SJ, Yamada Y, *et al.* Impact of *p53* aberration on the progression of adult T-cell leukemia/lymphoma. *Cancer Lett* 2006;**234**:249–55.
12. Vassilev LT, Vu BT, Graves B, *et al.* In vivo activation of the p53 pathway b small-molecule antagonists of MDM2. *Science* 2004;**303**:844–8.
13. Yamada Y, Sugawara K, Hata T, *et al.* Interleukin-15 (IL-15) can replace the IL-2 signal in IL-2-dependent adult T-cell leukemia (ATL) cell lines: expression of IL-15 receptor alpha on ATL cells. *Blood* 1998;**91**:4265–72.
14. Untergasser A, Nijveen H, Rao X, Bisseling T, Geurts R, Leunissen LKM. Primer3Plus, an enhanced web interface to Primer3. *Nucleic Acids Res* 2007;**35**:71–74. web service issue, doi:10.1093/nar/gkm306
15. Hasegawa H, Yamada Y, Komiyama K, *et al.* Dihydroflavonol BB-1, an extract of natural plant Blumea balsamifera, abrogates TRAIL resistance in leukemia cells. *Blood* 2006;**107**:679–88.
16. Wada M, Bartram CR, Nakamura H, *et al.* Analysis of *p53* mutations in a large series of lymphoid hematologic malignancies of childhood. *Blood* 1993;**82**:3163–9.
17. Hollstein M, Rice K, Greenblatt MS, Soussi T, Fuchs R, Sorlie T, Hovig E, Smith-Sorensen B, Montesano B, Harris CC. Database of p53 gene somatic mutations in human tumors and cell lines. *Nucleic Acids Res* 1994;**22**:3551–5.
18. Prokocimer M, Unger R, Rennert HS, Rotter V, Rennert G. Pooled analysis of *p53* mutations in hematological malignancies. *Hum Mutat* 1998;**12**:4–18.
19. Nelson HH, Wilkojmen M, Marsit CJ, Kelsey KT. TP53 mutation, allelism and survival in non-small cell lung cancer. *Carcinogenesis* 2005;**26**:1770–3.
20. Yatabe Y, Konishi H, Mitsudome T, Nakamura S, Takahashi T. Topographical distributions of allelic loss in individual non-small cell lung cancers. *Am J Pathol* 2000;**157**:985–93.
21. Baumbusch LO, Myhre S, Langerod A, Bergamaschi A, Geisler SB, Lonning PE, Deppert W, Dornreiter I, Borresen-Dale AL. Expression of full-length p53 and its isoform delta-p53 in breast carcinomas in relation to mutation status and clinical parameters. *Mol Cancer* 2006;**5**:47 http://www.molecular-cancer.com/content/51/47.
22. Yins Y, Charles W, Stephenst M, Lucianis G, Fahraeuss R. *p53* stability and activity is regulated by Mdm2-mediated induction of alternative p53 translation products. *Nat Cell Biol* 2002;**4**:462–7.
23. Mills AA. *p53*: link to the past, bridge to the future. *Genes Dev* 2005;**19**:2091–9.
24. Walker DR, Bond JP, Tarone RE, Harris CC, Makalowski W, Boguski MS, Greenblatt MS. Evolutionary conservation and somatic mutation hotspot maps of *p53*: correlation with p53 protein structural and functional features. *Oncogene* 1999;**19**:211–8.

Original Paper

Intervirology

Intervirology 2009;52:115–122
DOI: 10.1159/000219384

Received: August 20, 2008
Accepted: March 25, 2009
Published online: May 20, 2009

Proviral Loads and Clonal Expansion of HTLV-1-Infected Cells following Vertical Transmission: A 10-Year Follow-Up of Children in Jamaica

Kazumi Umeki[a] Michie Hisada[b] Elizabeth M. Maloney[c] Barrie Hanchard[d]
Akihiko Okayama[a]

[a]Department of Rheumatology, Infectious Diseases and Laboratory Medicine, University of Miyazaki, Miyazaki, Japan; [b]Division of Cancer Epidemiology and Genetics, NCI, Rockville, Ind., and [c]Centers for Disease Control and Prevention, Atlanta, Ga., USA; [d]Department of Pathology, University of the West Indies, Mona, Jamaica

Key Words
HTLV-1 infection · Clonal expansion, infected cells · Transmission, vertical

Abstract
Objective: Few studies have specifically examined proviral load (PVL) and clonal evolution of human T-lymphotropic virus type 1 (HTLV-1)-infected cells in vertically infected children. ***Methods:*** Sequential samples (from ages 1 to 16 years) from 3 HTLV-1-infected children (cases A, B and C) in the Jamaica Mother Infant Cohort Study were analyzed for their PVL and clonal expansion of HTLV-1-infected cells in peripheral blood mononuclear cells (PBMCs) by inverse-long PCR. ***Results:*** The baseline PVL (per 100,000 PBMCs) of case A was 260 (at 1 year of age) and of case B it was 1,867 (at 3 years of age), and they remained constant for more than 10 years. Stochastic patterns of clonal expansion of HTLV-1-infected cells were predominately detected. In contrast, case C, who had lymphadenopathy, seborrheic dermatitis and hyperreflexia, showed an increase in PVL from 2,819 at 1.9 years to 13,358 at 13 years of age, and expansion of 2 dominant clones. ***Conclusion:*** The clonal expansion of HTLV-1-infected cells is induced in early childhood after infection acquired from their mothers. Youths with high PVL and any signs and symptoms associated with HTLV-1 infection should be closely monitored.

Introduction

Human T-lymphotropic virus type 1 (HTLV-1) is a causative agent of adult T-cell leukemia/lymphoma (ATL) and a progressive neurological disease known as HTLV-1-associated myelopathy/tropical spastic paraparesis [1–3]. The majority of HTLV-1 carriers are asymptomatic, and only a fraction of carriers develop ATL after a long latent period [4, 5]. High proviral load (PVL) has been considered to be important for developing ATL. It has been shown that PVL vary substantially among adult HTLV-1 carriers, whereas within the same individual, PVL appears to remain relatively stable for many years [6–8]. Most mothers of patients with ATL are themselves HTLV-1 carriers [9, 10]. Therefore, ATL is believed to develop in HTLV-1 carriers who acquired infection perinatally. A study in perinatally infected children demonstrated variation of initial PVL [11]. In children with

KARGER

Fax +41 61 306 12 34
E-Mail karger@karger.ch
www.karger.com

Accessible online at:
www.karger.com/int

Akihiko Okayama, MD, PhD
Department of Rheumatology, Infectious Diseases and Laboratory Medicine
Faculty of Medicine, University of Miyazaki
5200 Kihara, Kiyotake, Miyazaki 889-1692 (Japan)
Tel. +81 985 7284, Fax +81 985 85 4709, E-Mail okayama@med.miyazaki-u.ac.jp

Table 1. Clinical signs and symptoms observed in case C

Age (years)	Clinical signs and symptoms
0.5	Inguinal lymphadenopathy
2.0	Abnormal lymphocyte finding (2%)
5.5	Seborrheic dermatitis
6.0	Eczema, axillary lymphadenopathy
6.5	Inguinal lymphadenopathy
8.5	Axillary lymphadenopathy
9.0	Persistent hyperreflexia, posterior cervical lymphadenopathy
9.5	Inguinal lymphadenopathy
10.0	Inguinal lymphadenopathy (diameter 2 cm)
16.0	No particular symptom

HTLV-1 infection, the association of infective dermatitis and seborrheic dermatitis is documented [12, 13]. The HTLV-1 carrier children with these skin manifestations have been reported to have high PVL in their peripheral blood mononuclear cells (PBMCs) [11, 14]. Moreover, epidemiological data have suggested that infective dermatitis might foreshadow ATL and HTLV-1-associated myelopathy/tropical spastic paraparesis [15, 16].

It is thought that HTLV-1 Tax protein drives proliferation of the infected cells, leading to the clonal expansion of certain HTLV-1-infected cells, which subsequently results in onset of ATL [6, 17–19]. It is uncertain whether and when such clonal expansion occurs in relation to PVL among children who acquire infection perinatally. To investigate the co-evolution of HTLV-1-infected clones and PVL during the early years of HTLV-1 infection in children, we analyzed sequential samples drawn from 3 children carrying HTLV-1 who were longitudinally followed for over 10 years.

Materials and Methods

Cases

The sequential samples of PBMCs obtained from 3 children carrying HTLV-1 (cases A, B and C) in the Jamaica Mother Infant Cohort Study [20] were tested. Informed consent was obtained from study participants, and the study was approved by the institutional review boards at the University of the West Indies, the US National Cancer Institute and University of Miyazaki. These children were born to mothers positive for HTLV-1 and had been followed for over 10 years since birth. One case with sufficient specimen volume and duration of follow-up was selected from each of the 3 groups of children with low, medium or high provirus load. Cases A and B (low and medium provirus load) were asymptomatic. Case C (the child with high provirus load) was selected based on the presence of clinical manifestations that included recurring history of lymphadenopathy, seborrheic dermatitis, and hyperreflexia since the patient was less than 1 year old (table 1). A low level of abnormal lymphocytes (2%) was seen in case C at 2 years of age, but not at other ages.

Quantification of HTLV-1 Provirus in PBMCs

The chromosomal DNA was isolated from PBMCs by sodium dodecyl sulfate-protease K digestion, followed by phenol-chloroform extraction and ethanol precipitation [21]. PVLs were measured by real-time PCR using LightCycler DX 400 (Roche Diagnostics, Mannheim, Germany). The primers and the probe for HTLV-1 provirus were as follows: forward primer 5′-AACCAATTCATTCAAACATCTGACC-3′, positions 3735–3759; reverse primer 5′-GCTTTCACAGGAGCCAATGG-3′, positions 3877–3858, and FAM-labeled probe 5′-FAM-TGTTCCTATCTTACTCCACCACAGTCACCGA-TAMRA-3′, positions 3767–3797. The nucleotide position number of HTLV-1 provirus was according to Seiki et al. (accession No. J02029) [22]. RNase P control reagent (Applied Biosystems, Foster City, Calif., USA) was used for the primers and the probe for human RNase P DNA as internal control. PVL was shown by the copy number of HTLV-1 provirus in 100,000 PBMCs.

Analysis of the Pattern of HTLV-1 Proviral Integration by Inverse Long PCR

A detailed description of the inverse long (IL)-PCR procedure has been provided elsewhere [6]. In brief, the genomic DNA was digested with *Eco*RI, self-ligated by T4 ligase, and then digested with *Mlu*I. Long PCR amplification of the resultant DNA was performed using the r*Tth* DNA polymerase (Applied Biosystems). The primers used in this analysis were primer 1 in the U5 region of the long terminal repeat (LTR) 5′-TGCCTGACCCTGCTTGCTCAACTCTACGTCTTTG-3′ (positions 8856–8889), and primer 2 in the U3 region of the LTR 5′-AGTCTGGGCCCTGACCTTTTCAGACTTCTGTTTC-3′ (positions 123–90). The PCR products were electrophoresed on a 1.2% agarose gel, and visualized by ethidium bromide staining. All assays were performed in triplicates.

Clone-Specific PCR for the Major Clones in Case C at Age 16 Years

When PBMCs of case C were analyzed by IL-PCR, 2 major bands were shown, at ages of 13 and 16 years (clone S 0.75 kb and clone L 4 kb). The proviral integration sites of these clones were identified as follows. DNAs of these 2 bands in case C at 16 years of age were isolated from the gel and ligated with the pCR-XL-TOPO vector using TOPO cloning reaction kit (Invitrogen, Carlsbad, Calif., USA). The DNA sequences of the cloned PCR products were analyzed using the ABI Prism Big Dye Terminator v1.1 Cycle Sequencing kit and an ABI Prism 310 genetic analyzer (Applied Biosystems). Based on the DNA sequence of the flanking region of the provirus derived from clones S and L, integration site-specific primers were designed. Accordingly, DNAs isolated from PBMCs of case C at 16 years of age were subjected to quantitative real-time PCR for clones S and L. Forward primer 5′-CCAAGTACCGGCGACTCC-3′ (positions 8976–8993) and probe FAM-CTCGGAGCCAGCGACAGCCTATCCT-TAMRA (positions 8999–9023) located in the U5 region of the LTR were

used. The reverse primers for specific clones were as follows: primer for clone S: 5′-CAACTTTGTTCTTTCAGACAGTGTG-3′; primer for clone L: 5′-CTGTTTCTCCCTCTTGAACTCTCC-3′. The copy number of the plasmid containing the DNA sequences of the cloned PCR products was calculated based on the size and weight of the plasmid DNA measured by spectrophotometry and used as a standard calibration curve.

Amplification of the Rearranged T Cell Receptor-γ Gene of the PBMCs in Case C at Age 16 Years

The rearrangement of the T cell receptor-γ (TCRγ) gene was detected by PCR described by Benhattar et al. [23], using primers TVG 5′-AGGGTTGTGTTGGAATCAGG-3′ and TJG 5′-CGTCGACAACAAGTGTTGTTCCAC-3′. Amplified products were electrophoresed on a 10% nondenaturing polyacrylamide gel, and visualized by ethidium bromide staining. Clonally rearranged TCRγ gene was identified based on the sharp and dominant band on the gel. Additionally, the PCR products were subcloned and sequenced using TOPO XL PCR Kit (Invitrogen), Big Dye Terminator v1.1 Cycle Sequencing Kit (Applied Biosystems), and ABI Prism 310 DNA Sequencer (Applied Biosystems).

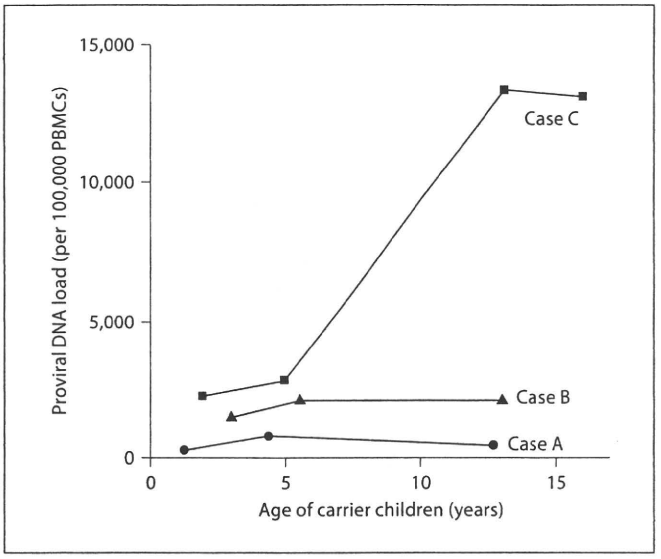

Fig. 1. Sequential change of the HTLV-1 proviral loads in the genomic DNA derived from 100,000 PBMCs of 3 carrier children.

Results

Sequential Change of HTLV-1 Proviral Loads and Clonalities of Infected Cells

The PVLs in cases A and B remained stable during the entire follow-up period (case A: 260, 850 and 573 copies in 100,000 PBMCs at ages of 1, 4.5, and 12.8 years, respectively; case B: 1,867, 2,199 and 2,187 copies in 100,000 PBMCs at ages 3, 5.6 and 13.1 years, respectively; fig. 1). When the PBMCs were analyzed by IL-PCR, case A demonstrated many bands of various sizes in the sample drawn at age 1 year. These bands represented HTLV-1-infected cells with different proviral integration sites. They appeared in a stochastic manner in the triplicate experiments shown on the gel (minor bands; fig. 2a). This stochasticity was also observed for this case's samples obtained at ages of 4.5 and 12.8 years. No band was consistently detected at different time points. In case B, who had a slightly higher PVL than case A, several bands were detected in all triplicate experiments of IL-PCR (major bands; arrows, fig. 2b), in addition to the minor bands. These major bands were also detectable in the samples obtained at ages of 5.6 and 13.1 years.

Case C had a history of recurring lymphadenopathy, seborrheic dermatitis, and hyperreflexia since early childhood (table 1). The initial PVL in case C was the highest among the 3 children, even at ages 1.9 and 5 years (2,819 and 3,005 copies per 100,000 PBMCs, respectively). The PVL in case C markedly increased to 13,358 copies in 100,000 PBMCs at age 13 years and remained high (13,185 copies per 100,000 PBMCs) at age 16 years (fig. 1).

When PBMCs of case C were analyzed by IL-PCR, 2 distinct bands were detected in samples drawn at ages 13 and 16 years (clone S 0.75 kb and clone L 4 kb; fig. 2c). Many additional major bands, albeit weaker in band strength, were detectable in the triplicate experiments in same samples.

Clone-Specific PCR and Quantification of the PVL for Clones S and L from Case C

The integration sites of HTLV-1 provirus for PCR products of clones S and L were isolated from the gel, subcloned and excised for the identification of proviral integration sites. Clones S and L were identified at 8q22.1 and 15q21.2, respectively. HTLV-1 provirus of clone S was integrated into the transcriptional unit of the gene for phosphatidylserine synthase 1 *(PTDSS1)* located on chromosome 8 in the opposite direction of the cellular gene (data not shown). Integration-site-specific real-time PCR was performed using a combination of primers specific for the 3′-LTR of provirus and its flanking regions based on their DNA sequences. DNA sequences of clones S and L were not detectable in the sample collected at 1.9 years of age by the clone-specific real-time PCR we used. These clones were detected as 5 copies and 230 copies in 100,000 PBMCs, respectively, in a sample collected at 5 years of age (fig. 3). Copy numbers of clones S and L increased at

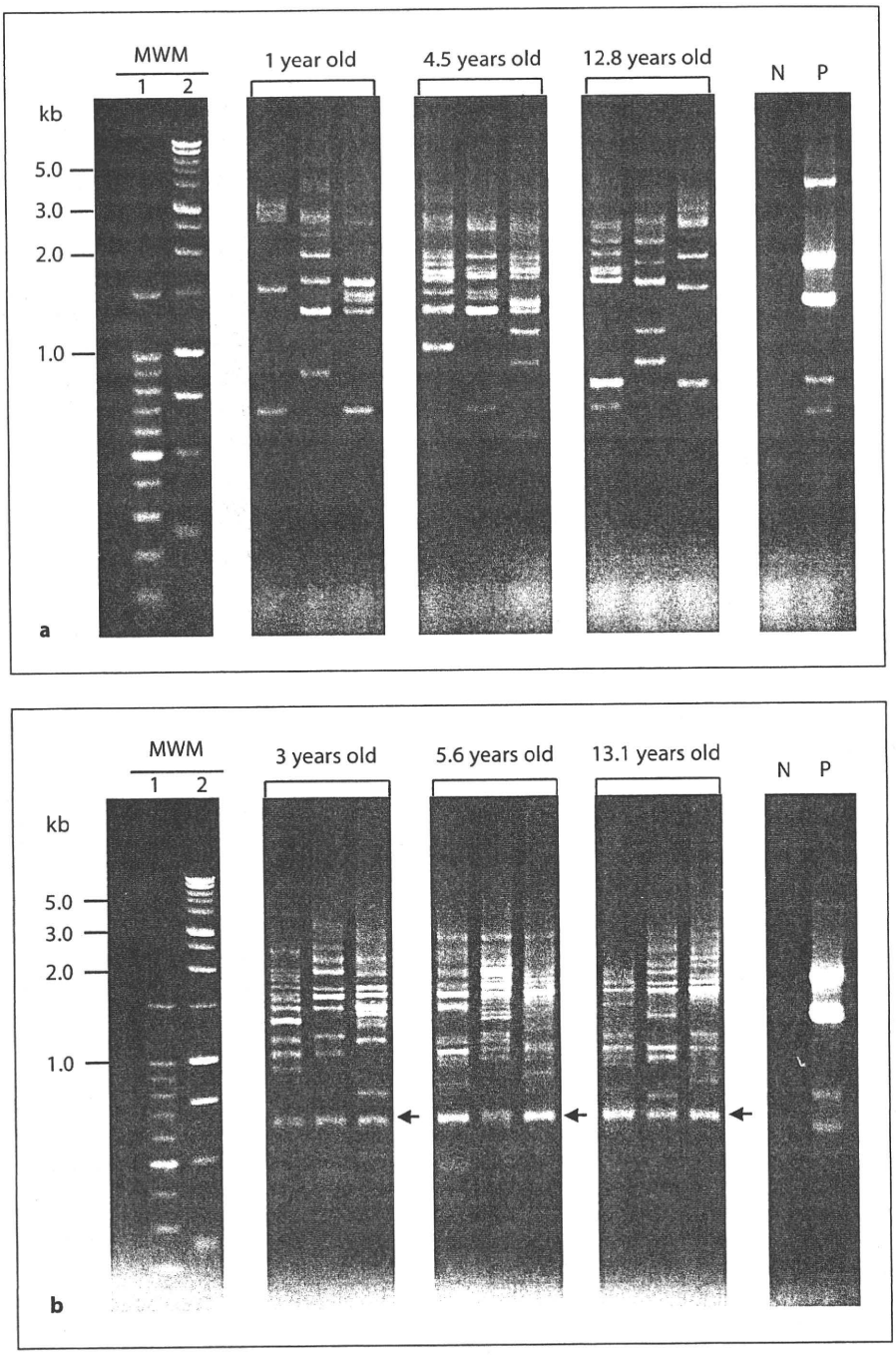

Fig. 2. Inverse long PCR analysis of HTLV-1-infected cells from carrier children. Triplicate analysis of PBMCs was performed in each experiment. MWM 1 = Low-molecular-weight DNA marker; MWM 2 = high-molecular-weight DNA marker; N = PBMCs from HTLV-1-negative subject as negative control; P = HTLV-1-infected cell line, HUT102, as positive control. **a** Analysis of case A at ages 1, 4.5 and 12.8 years. **b** Analysis of case B at ages 3, 5.6 and 13.1 years. Arrows indicate the bands detected in all triplicate analyses.

ages 13 (426 and 554 copies, respectively) and 16 years (768 and 594 copies, respectively).

Rearrangement of the TCRγ Gene of PBMCs in Case C

Whether or not the rearrangement of the TCRγ gene was detectable by PCR was tested in the sample of case C at age 16 years. Detection of a weak but sharp band (arrow in fig. 4) suggested the clonal expansion of the cells with the rearranged TCRγ gene. To confirm the clonal expansion of certain clones of T cells, PCR products of the TCRγ gene were subcloned and sequenced. The frequency of PCR products derived from the clones of T cells with a unique (different) TCRγ gene in the sample of case C at

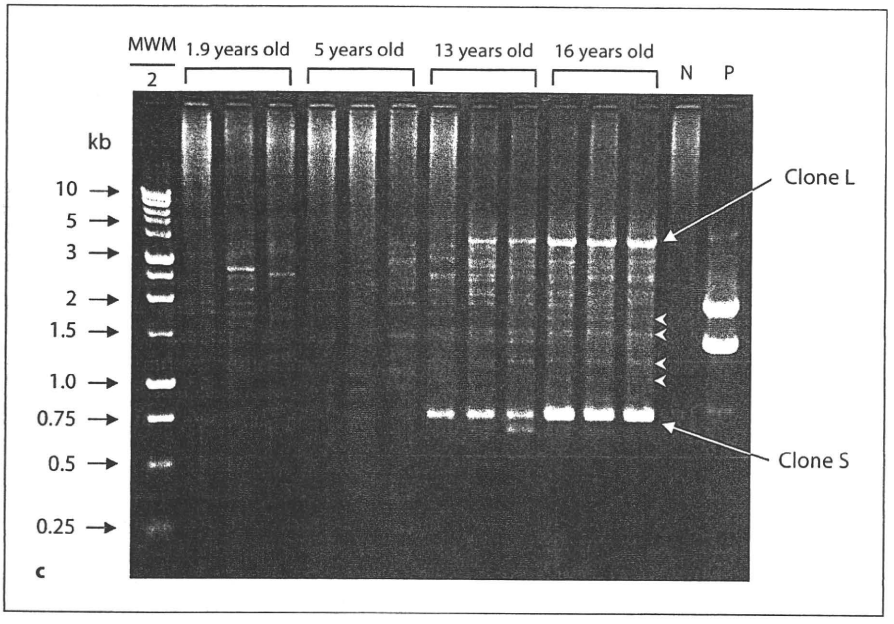

Fig. 2. c Analysis of case C at ages 1.9, 5, 13 and 16 years. Arrows indicate 2 distinct bands (clone S and L) detected in all triplicate analyses. Arrowheads indicate the week but consistently detected bands in all triplicate analyses.

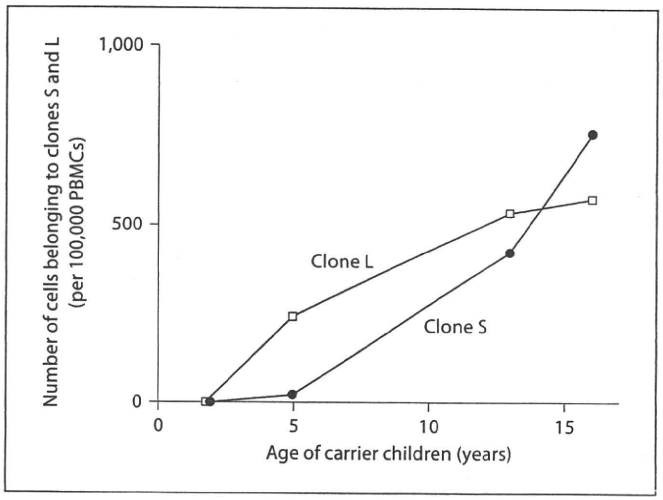

3

Fig. 3. Sequential change of the copy numbers of clones S and L in case C in 100,000 PBMCs at ages 1.9, 5, 13 and 16 years. Clone-specific quantitative real-time PCR was performed.

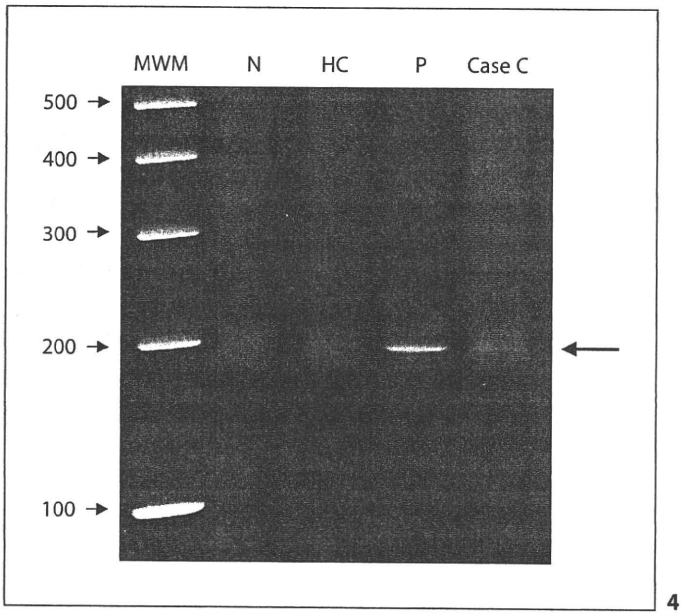

4

Fig. 4. Polymerase chain reaction analysis of the rearrangements of TCRγ gene in case C at age 16 years. N = PBMCs from a healthy volunteer not infected with HTLV-1 and who is not involved in this cohort, as a negative control; HC = PBMCs from an HTLV-1 carrier, who is not involved in this cohort, as an HTLV-1-positive control; P = a patient with adult T cell leukemia, who is not involved in this cohort, showing a sharp and dominant band, as positive control; case C = PBMCs from case C at age 16 years old, who showed a weak, but evident band in a smear background (arrow).

age 16 years was assessed in the resulting 128 subclones. Among 128 subclones, 5 major clones (fig. 5, closed symbols and double circles) with the same lengths and DNA sequences were repeatedly detectable in the background of minor clones (fig. 5, open circles). Each minor clone was detectable only once and exhibited different DNA sequences (fig. 5). These data confirmed the oligoclonal expansion of T cells in the PBMCs of case C at age 16 years.

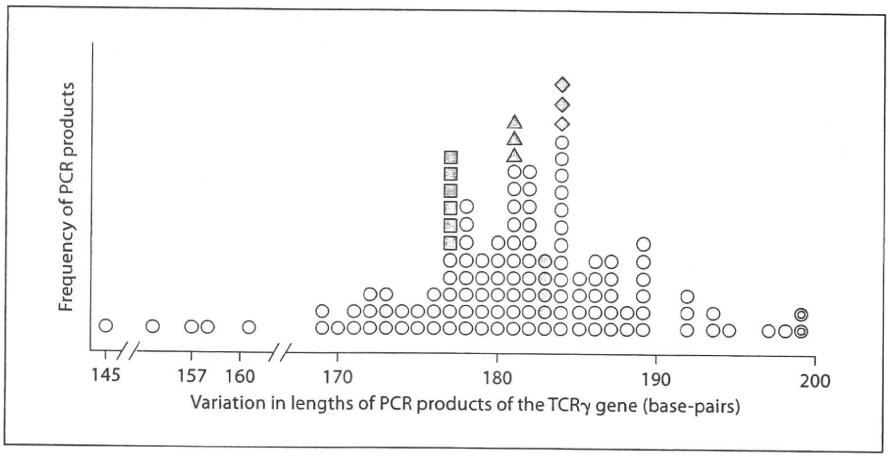

Fig. 5. Distribution of 128 subclones of the polymerase chain reaction (PCR) products of TCRγ gene in case C at age 16 years based on their variation in lengths. Each open circle indicates a unique PCR product, showing the diversity in the length and the DNA sequence. The 5 groups of PCR products indicated by the closed square, triangle, circle, diamond, and double circle indicate the clones detected repeatedly and showed identical DNA sequences.

Discussion

In the present study, 3 carrier children, who were longitudinally followed for more than 10 years, were tested for PVL and clonality of HTLV-1-infected cells. This study gave us a unique opportunity to evaluate the HTLV-1 infection early in the life. Two asymptomatic carrier children (cases A and B) showed stable PVL and 1 carrier child (case C), who experienced lymphadenopathy, seborrheic dermatitis and hyperreflexia, showed a prominent increase of PVL. In a previous publication, we described the pattern of changes in PVL of 28 children, including the 3 in the current analysis [11]. PVL in these vertically infected children increased up to 2 years after infection and plateaued thereafter, with an increase to a much higher PVL observed in the HTLV-1 carrier children with a diagnosis of eczema [11]. Gabet et al. [24] also reported the case of a 10-year-old girl, who was followed over a 2-year period, with infective dermatitis and infection with parasites. She had high PVLs and extensive and persistent oligoclonal expansion of infected lymphocytes, which was not influenced by clinical evolution or lamivudine treatment [24].

In the present study, when the clonality of HTLV-1-infected cells was examined by IL-PCR, many bands of different sizes appeared on the gel for case A, who had relatively low PVL, representing polyclonal proliferation of HTLV-1-infected cells. Case B with relatively high PVL showed several major clones that were consistently detectable in the PBMC samples obtained at ages of 3, 5.6 and 13.1 years. The latter pattern was similar to that observed in the Japanese adult long-term carriers in the Miyazaki Cohort Study, who presumably were infected during the perinatal period [25]. These data are consistent with the hypothesis that clonal expansion may occur concurrently with increase in PVL.

Case C had a history of lymphadenopathy, seborrheic dermatitis and hyperreflexia. These symptoms and signs are not uncommon in the HTLV-1 carrier children in Jamaica [14]. Case C showed a very high PVL and 2 distinct clones (S and L) of HTLV-1-infected cells at age 13 years. The appearance of these clones coincided with a sharp increase in PVL between the ages of 5 and 13 years. DNA sequences of clones S and L were detectable by real-time PCR in case C's sample as early as 5 years of age and expanded continuously to 426 and 554 copies in 100,000 PBMCs, respectively, at 13 years of age. However, these 2 clones only accounted for less than 10% of the total PVL of case C (13,358 copies in 100,000 PBMCs). Many additional major bands were observed on the gel of the sample at the same age. Therefore, the marked increase of PVL in case C was considered to be due to the sum of these clones, although clone S and clone L were very evident.

It has been reported that HTLV-1 provirus is randomly integrated into the human genome. Nevertheless, proviral DNA sequences found in the ATL cells have been reported to be preferentially integrated into transcriptional units [26, 27]. It was thought that parts of corresponding genes are dysregulated, leading to proliferation of HTLV-1-infected cells. Expansion of clone S may be associated with the interaction between HTLV-1 provirus and host gene *PTDSS1*. However, proviral DNA of clone L was not integrated into the transcriptional unit. These findings suggest that integration of proviral DNA into transcriptional units is not essential for the occurrence of clonal expansion.

The high PVL and detection of 2 distinct clones of HTLV-1-infected cells in case C were also evident at age

16 years, 3 years later. The analysis of the TCRγ gene rearrangement, which does not depend on HTLV-1 proviral integration, also detected an oligoclonal expansion of 5 T cell clones, which were repeatedly detected by PCR in the background of many T cells without clonality. The occurrence of ATL in patients with a history of infective dermatitis was reported [15]. The shortened period of latency was observed in ATL patients with chronic infection, such as strongyloidiasis [28]. Fortunately, case C did not show any signs of HTLV-1-associated disease, especially ATL, at age 16 years. Our data suggest that detection of clonal expansion of HTLV-1-infected cells does not always indicate the onset of clinically evident ATL. However, continuous clinical monitoring is warranted in this case, for any early signs of HTLV-1-associated disease.

Active HTLV-1 infection may have resulted in lymphadenopathy and inflammatory diseases in case C. Alternatively, these inflammatory diseases in childhood may have stimulated the immune system of case C, resulting in the expansion of certain T cells. If these activated T cells were infected with HTLV-1, DNA sequences of HTLV-1 provirus, especially the Tax-coding region, could have been transcribed at the same time. Therefore, it is possible that inflammatory antigenic stimulation, such as co-infection of other pathogens or allergic diseases in childhood, may induce the early clonal expansion of HTLV-1-infected T cells, leading to eventual development of ATL. The findings from the present study are suggestive, but warrant further study that includes larger number of cases.

Children infected with HTLV-1 during early childhood have an increased risk of developing ATL [9, 10]. In the present study, high PVL and the clonal expansion of HTLV-1-infected cells were seen in 2 of 3 children who were infected from their mothers. The clonal expansion accompanied by high PVL was most evident in a child who had skin manifestations. Youths with high PVL should be carefully monitored for any signs and symptoms, because the concurrent presence of high PVL and skin manifestations in carrier children could represent underlying oligoclonal expansion of clones, and thus future risk for clinically overt HTLV-1-associated diseases [29].

Acknowledgments

We thank Mrs. Beverley Granston for her contribution to the study conduct. This study was supported in part by a grant-in-aid from the Japanese Ministry of Education, Science, Sports and Culture, and the Miyazaki Prefecture Collaboration of Regional Entities for the Advancement of Technological Excellence (JST). The Jamaica Mother Infant Cohort Study was supported by the Intramural Research Program of the NIH, National Cancer Institute, Division of Cancer Epidemiology and Genetics.

References

1 Uchiyama T, Yodoi J, Sagawa K, Takatsuki K, Uchino H: Adult T-cell leukemia: clinical and hematologic features of 16 cases. Blood 1977;50:481–492.

2 Yoshida M, Miyoshi I, Hinuma Y: Isolation and characterization of retrovirus from cell lines of human adult T-cell leukemia and its imolication in the disease. Proc Natl Acad Sci USA 1982;79:2031–2035.

3 Osame M, Usuku K, Izumo S, Ijichi N, Amitani H, Igata A, Matsumoto M, Tara M: HTLV-I associated myelopathy, a new clinical entity. Lancet 1986;1:1031–1032.

4 Arisawa K, Soda M, Endo S, Kurokawa K, Katamine S, Shimokawa I, Koba T, Takahashi T, Saito H, Doi H, Shirahama S: Evaluation of adult T-cell leukemia/lymphoma incidence and its impact on non-Hodgkin lymphoma incidence in southwestern Japan. Int J Cancer 2000;85:319–324.

5 Yamaguchi K, Watanabe T: Human T lymphotropic virus type-I and adult T-cell leukemia in Japan. Int J Hematol 2002;76:240–245.

6 Etoh K, Tamiya S, Yamaguchi K, Okayama A, Tsubouchi H, Ideta T, Mueller N, Takatsuki K, Matsuoka M: Persistent clonal proliferation of human T-lymphotropic virus type I-infected cells in vivo. Cancer Res 1997;57:4862–4867.

7 Etoh K, Yamaguchi K, Tokudome S, Watanabe T, Okayama A, Stuver S, Mueller N, Takatsuki K, Matsuoka M: Rapid quantification of HTLV-I provirus load: detection of monoclonal proliferation of HTLV-I-infected cells among blood donors. Int J Cancer 1999;81:856–864.

8 Okayama A, Stuver S, Iga M, Okamoto M, Mueller N, Matsuoka M, Yamaguchi K, Tachibana N, Tsubouchi H: Sequential change of virus markers in seroconverters with community-acquired infection of human T lymphotropic virus type I. J Infect Dis 2001;183:1031–1037.

9 Wilks R, Hanchard B, Morgan O, Williams E, Cranston B, Smith ML, Rodgers-Johnson P, Manns A: Patterns of HTLV-I infection among family members of patients with adult T-cell leukemia/lymphoma and HTLV-I associated myelopathy/tropical spastic paraparesis. Int J Cancer 1996;65:272–273.

10 Bartholomew C, Jack N, Edwards J, Charles W, Corbin D, Cleghorn FR, Blattner WA: HTLV-I serostatus of mothers of patients with adult T-cell leukemia and HTLV-I-associated myelopathy/tropical spastic paraparesis. J Hum Virol 1998;1:302–305.

11 Maloney EM, Yamano Y, Vanveldhuisen PC, Sawada T, Kim N, Cranston B, Hanchard B, Jacobson S, Hisada M: Natural history of viral markers in children infected with human T lymphotropic virus type I in Jamaica. J Infect Dis 2006;194:552–560.

12 LaGrenade L, Hanchard B, Fletcher V, Cranston B, Blattner W: Infective dermatitis of Jamaican children: a marker for HTLV-I infection. Lancet 1990;336:1345–1347.

13 Maloney EM, Nagai M, Hisada M, Soldan SS, Goebel PB, Carrington M, Sawada T, Brennan MB, Cranston B, Hanchard B, Jacobson S: Prediagnostic human T lymphotropic virus type I provirus loads were highest in Jamaican children who developed seborrheic dermatitis and severe anemia. J Infect Dis 2004;189:41–45.
14 Maloney EM, Wiktor SZ, Palmer P, Cranston B, Pate EJ, Cohn S, Kim N, Miley W, Thomas TL, Blattner WA, Hanchard B: A cohort study of health effects of human T-cell lymphotropic virus type I infection in Jamaican children. Pediatrics 2003;112:e136–e142.
15 Hanchard B, LaGrenade L, Carberry C, Fletcher V, Williams E, Cranston B, Blattner WA, Manns A: Childhood infective dermatitis evolving into adult T-cell leukaemia after 17 years. Lancet 1991;338:1593–1594.
16 La Grenade L: HTLV-I-associated infective dermatitis: past, present, and future. J Acquir Immune Defic Syndr Hum Retrovirol 1996;13(suppl 1):S46–S49.
17 Yoshida M: Multiple viral strategies of HTLV-1 for dysregulation of cell growth control. Annu Rev Immunol 2001;19:475–496.
18 Okayama A, Stuver S, Matsuoka M, Ishizaki J, Tanaka G, Kubuki Y, Mueller N, Hsieh CC, Tachibana N, Tsubouchi H: Role of HTLV-1 proviral DNA load and clonality in the development of adult T-cell leukemia/lymphoma in asymptomatic carriers. Int J Cancer 2004;110:621–625.
19 Cavrois M, Leclercq I, Gout O, Gessain A, Wain-Hobson S, Wattel E: Persistent oligoclonal expansion of human T-cell leukemia virus type 1-infected circulating cells in patients with tropical spastic paraparesis/HTLV-1 associated myelopathy. Oncogene 1998;17:77–82.
20 Wiktor SZ, Pate EJ, Rosenberg PS, Barnett M, Palmer P, Medeiros D, Maloney EM, Blattner WA: Mother-to-child transmission of human T-cell lymphotropic virus type I associated with prolonged breast-feeding. J Hum Virol 1997;1:37–44.
21 Sambrook J, Russell DW: Molecular cloning: a laboratory manual, 3rd ed. New York, Cold Spring Harbor Laboratory Press, 2001, pp 6.4–11p.
22 Seiki M, Hattori S, Hirayama Y, Yoshida M: Human adult T-cell leukemia virus: complete nucleotide sequence of the provirus genome integrated in leukemia cell DNA. Proc Natl Acad Sci USA 1983;80:3618–3622.
23 Benhattar J, Delacretaz F, Martin P, Chaubert P, Costa J: Improved polymerase chain reaction detection of clonal T-cell lymphoid neoplasms. Diagn Mol Pathol 1995;4:108–112.
24 Gabet AS, Kazanji M, Couppie P, Clity E, Pouliquen JF, Sainte-Marie D, Aznar C, Wattel E: Adult T-cell leukaemia/lymphoma-like human T-cell leukaemia virus-1 replication in infective dermatitis. Br J Haematol 2003;123:406–412.
25 Tanaka G, Okayama A, Watanabe T, Aizawa S, Stuver S, Mueller N, Hsieh CC, Tsubouchi H: The clonal expansion of human T lymphotropic virus type 1-infected T cells: a comparison between seroconverters and long-term carriers. J Infect Dis 2005;191:1140–1147.
26 Ozawa T, Itoyama T, Sadamori N, Yamada Y, Hata T, Tomonaga M, Isobe M: Rapid isolation of viral integration site reveals frequent integration of HTLV-1 into expressed loci. J Hum Genet 2004;49:154–165.
27 Hanai S, Nitta T, Shoda M, Tanaka M, Iso N, Mizoguchi I, Yashiki S, Sonida S: Integration of human T-cell leukemia virus type 1 in genes of leukemia cells of patients with adult T-cell leukemia. Cancer Sci 2004;95:306–310.
28 Plumelle Y, Gonin C, Edouard A, Bucher BJ, Thomas L, Brebion A, Panelatti G: Effect of *Strongyloides stercoralis* infection and eosinophilia on age at onset and prognosis of adult T-cell leukemia. Am J Clin Pathol 1997;107:81–87.
29 Farre L, de Oliveira Mde F, Primo J, Vandamme AM, Van Weyenbergh J, Bittencourt AL: Early sequential development of infective dermatitis, human T cell lymphotropic virus type 1-associated myelopathy, and adult T cell leukemia/lymphoma. Clin Infect Dis 2008;46:440–442.

Int. J. Cancer: **124,** 614–621 (2009)

Population differences in immune marker profiles associated with human T-lymphotropic virus type I infection in Japan and Jamaica

Brenda M. Birmann[1]*, Elizabeth C. Breen[2], Sherri Stuver[1,3], Beverly Cranston[4], Otoniel Martínez-Maza[2], Kerstin I. Falk[5], Akihiko Okayama[6], Barrie Hanchard[4], Nancy Mueller[1] and Michie Hisada[7]

[1]*Department of Epidemiology, Harvard School of Public Health, Boston, MA*
[2]*Department of Obstetrics and Gynecology and Microbiology, Immunology and Molecular Genetics, David Geffen School of Medicine, University of California Los Angeles, Los Angeles, CA*
[3]*Department of Epidemiology, Boston University School of Public Health, Boston, MA*
[4]*Department of Pathology, University of the West Indies, Kingston, Jamaica*
[5]*Centre for Microbiological Preparedness, Swedish Institute for Infectious Disease Control and Department of Microbiology, Tumor and Cell Biology, Karolinska Institute, Stockholm, Sweden*
[6]*Department of Laboratory Medicine, Miyazaki Medical College, University of Miyazaki, Kiyotake, Miyazaki, Japan*
[7]*Viral Epidemiology Branch, Division of Cancer Epidemiology and Genetics, National Cancer Institute, National Institutes of Health, Department of Health and Human Services, Bethesda, MD*

The natural history of human T-lymphotropic virus type I (HTLV-I) has been shown to differ markedly by geographic area. The differences include contrasting patterns of risk of adult T-cell lymphoma (ATL) and HTLV-I-associated myelopathy/tropical spastic paraparesis (HAM/TSP), which may be due in part to differences in host immune response to infection. To characterize variations in host immunity across populations, we compared serologic immune marker patterns in HTLV-I-endemic populations in Japan and Jamaica. We matched 204 participants with archived blood from the Miyazaki Cohort Study (Japan) and the Food Handlers Study (Jamaica)—*i.e.*, 51 HTLV-I-positive ("carriers") and 51 HTLV-I-negative individuals ("noncarriers") from each population—by age, sex and blood collection year. We compared plasma concentrations of markers of T-cell-mediated (antigen-specific) and nonspecific immunity using regression models and correlation coefficients. Compared to Jamaican HTLV-I noncarriers, Japanese noncarriers had higher covariate-adjusted mean levels of T-cell activation markers, including antibody to Epstein-Barr virus nuclear antigen-1 (reciprocal titer 27 *vs.* 71, respectively, $p = 0.005$), soluble interleukin-2 receptor-α (477 *vs.* 623 pg/mL, $p = 0.0008$) and soluble CD30 (34 *vs.* 46 U/mL, $p = 0.0001$) and lower levels of C-reactive protein (1.1 *vs.* 0.43 μg/mL, $p = 0.0004$). HTLV-I infection was associated with activated T-cell immunity in Jamaicans but with diminished T-cell immunity in Japanese persons. The observed population differences in background and HTLV-I-related host immunity correspond closely to the divergent natural histories of infection observed among HTLV-I carriers in Japan and Jamaica and corroborate a role for host immune status in the contrasting patterns of ATL and HAM/TSP risk.

Key words: HTLV-I; epidemiology; natural history; host immunity; viral markers

Human T-lymphotropic virus type I (HTLV-I) is associated with adult T-cell lymphoma (ATL) and HTLV-I-associated myelopathy/tropical spastic paraparesis (HAM/TSP).[1] HTLV-I infection is endemic in southern Japan, the Caribbean and portions of South America, Africa, the Middle East and Melanesia.[1,2] The risk of ATL and HAM/TSP among individuals infected with HTLV-I ("carriers") varies markedly across Japanese and Caribbean populations. In Japanese carriers, the annual incidence of ATL is comparatively high, peaks around age 60 and is approximately 3 times greater in men than in women.[3,4] The incidence of ATL among Caribbean carriers is less than one-third the rate in Japan, peaks in the forties and does not vary by gender. In contrast, the incidence of HAM/TSP is relatively high among Caribbean carriers, whereas in Japan HAM/TSP occurs at one-tenth the rate in the Caribbean.[2,3] HAM/TSP demonstrates a female predominance in both populations.

Genetic variation of the virus does not explain the population differences in HTLV-I-related morbidity.[4,5] Instead, factors such as age at infection, route and dose of infection, nutritional status, social environment, co-morbidity and/or host genetics likely contribute to the geographic differences in natural history,[6] in part by influencing the initial host immune response to HTLV-I. For example, ATL appears to develop primarily in persons who acquire HTLV-I perinatally, whereas HAM/TSP often occurs in persons infected later in life.[2]

Efficient cellular immunity,[7] including an antigen-specific (*i.e.*, virus-specific) cytotoxic T-lymphocyte (CTL) and a type 1 cytokine response, is important for host control of most viral infections. Several serologic markers of HTLV-I pathogenesis (*i.e.* "viral markers") serve as indicators of the host immune response to HTLV-I. One viral marker is provirus load,[2,8,9] which represents the proportion of host peripheral blood mononuclear cells with integrated HTLV-I genome (*i.e.*, provirus). Antibodies against HTLV-I structural proteins (anti-HTLV-I), which are found in all HTLV-I carriers, serve as another viral marker and are considered indicative of viral protein expression and of the division of provirus-containing T-lymphocytes.[2,3,8] Antibody to Tax (anti-Tax), a product of the HTLV-I *tax* regulatory gene that can induce viral and host gene transcription,[2] is a third viral marker. Anti-Tax

Abbreviations: ATL, adult T-cell leukemia/lymphoma; CI, confidence interval; CRP, C-reactive protein; CTL, cytotoxic T-lymphocyte; EA, early antigen; EBNA, Epstein-Barr virus nuclear antigen; EBV, Epstein-Barr virus; ELISA, enzyme-linked immunosorbent assay; HAM/TSP, human T-lymphotropic virus-I-associated myelopathy/tropical spastic paraparesis; HTLV-I, human T-lymphotropic virus type I; IFA, immunofluorescence assay; IL, interleukin; IL-2R, IL-2 receptor-α; IgE, immunoglobulin E; OR, odds ratio; sCD30, soluble CD30; sIL2R, soluble IL-2R; VCA, viral capsid antigen.

Grant sponsor: Public Health Service; Grant numbers: CA115687, CA38450, CA09001. Grant sponsors: Intramural Research Program of the National Institutes of Health, National Cancer Institute, Division of Cancer Epidemiology and Genetics.

Elizabeth C. Breen's current address is: Cousins Center for Psychoneuroimmunology, Semel Institute for Neuroscience, Department of Psychiatry and Biobehavioral Sciences, David Geffen School of Medicine, University of California Los Angeles, Los Angeles, CA.

Michie Hisada's current address is: Takeda Global Research & Development Center, Inc., Deerfield, IL.

Nancy Mueller and Michie Hisada contributed equally to this work.

***Correspondence to:** Brenda M. Birmann's current address is: Channing Laboratory, Department of Medicine, Brigham and Women's Hospital and Harvard Medical School, 181 Longwood Avenue, Boston, MA 02115, USA. Fax: +617-525-2008.

E-mail: brenda.birmann@channing.harvard.edu

Received 25 March 2008; Accepted after revision 27 August 2008

DOI 10.1002/ijc.24012

Published online 19 September 2008 in Wiley InterScience (www.interscience.wiley.com).

Publication of the International Union Against Cancer

detection is associated with an active CTL response to HTLV-I; the absence of anti-Tax is considered to indicate a lack of Tax expression.[2] Of interest, anti-Tax is observed in HAM/TSP but not frequently in ATL patients.[10–12]

ATL patients are generally considered to have diminished cellular immunity[1,2]; patients from Japan had Epstein-Barr virus (EBV)-specific antibody responses suggestive of diminished cellular immunity[13] and increased expression of the cytokine transforming growth factor β_1.[14] In contrast to ATL, HAM/TSP is characterized by activated inflammatory and CTL responses to HTLV-I,[1,2] including upregulation of pro-inflammatory and type 1 cytokines.[6,14] Ultimately, differential CTL responses to HTLV-I, mediated in part by cytokines, are thought to be an important determinant of the contrasting population risks of ATL and HAM/TSP.

In a recent comparison of HTLV-I viral markers in asymptomatic carriers from Jamaica and Japan,[15] we observed similar mean provirus loads in both populations (3.0 *vs.* 3.1 $\log_{10}$ copies/10^5 cells, respectively, $p = 0.26$), but significantly higher mean anti-HTLV-I titer (3.6 *vs.* 3.2 $\log_{10}$ reciprocal titer, respectively, $p = 0.03$) and anti-Tax seroprevalence (59% *vs.* 39%, respectively, $p = 0.002$) in Jamaican than in Japanese carriers. Those viral marker patterns suggested that Jamaican carriers may have heightened anti-HTLV-I immunity and persistent HTLV-I replication, whereas Japanese carriers have mitotic proliferation of HTLV-I-infected T-lymphocytes in the absence of strong antiviral immunity.[15] Of interest, we[16–18] and others[13,19] have reported immune marker patterns suggestive of subclinical immune deficiency in HTLV-I carriers in Japan. However, the immune statuses of Jamaican and Japanese carriers have not been directly compared. We conducted the present study to perform the first direct comparison of immune status across these populations. Biospecimens appropriate for a direct assessment of antiviral CTL activity were not available. Thus, we tested a panel of plasma immune markers in the HTLV-I carriers from our virus marker study[15] and in HTLV-I-negative persons ("noncarriers") from the same study populations.[9,20] We also evaluated correlations between immune markers and levels of HTLV-I viral markers among carriers within each population.[15]

Material and methods

Study population

Japanese subjects were participants in the Miyazaki Cohort Study, a prospective study conducted among adult residents of 2 rural villages in Miyazaki Prefecture between 1984 and 2000 in conjunction with government-sponsored annual health examinations.[9] Jamaican individuals were participants in the Food Handlers Study,[20] a series of three cross-sectional surveys conducted between 1985 and 1993 among a total of 13,920 applicants for food-handling licenses from all Jamaican parishes. From these two populations, we had previously selected 51 pairs of Japanese and Jamaican HTLV-I carriers, matched by age (±2 years), sex and sample collection year (±2 years), for a comparison of HTLV-I viral markers.[15] For the present analysis, we randomly selected 1 HTLV-I noncarrier from within the same cohort for each of the 51 pairs of carriers, using the same matching criteria as for the carrier pairs. Thus, the analysis included 51 matched sets of 4 participants ($N = 204$) that comprised 1 carrier and 1 noncarrier from each study population. Blood samples from these subjects had been stored at −80°C in the respective repositories. The study protocol followed the human-experimentation guidelines of the US Department of Health and Human Services and received approval from the institutional review boards of each collaborating institution. Each participant provided informed consent.

HTLV-I viral markers

Laboratory methods to determine seropositivity for HTLV-I, quantify anti-HTLV-I titers, detect anti-Tax and quantify HTLV-I provirus load have been described previously.[11,15,21]

Immune markers

Matched sets of plasma samples were tested in the same batch for each assay, by technicians blinded to population and HTLV-I status. Plasma EBV antibodies were measured by immunofluorescence assay (IFA) techniques.[22–24] Titers were reported as the highest of serial 2-fold dilutions to yield a positive IFA reading.

Commercial enzyme-linked immunosorbent assays (ELISA) were performed according to manufacturer's instructions to quantify peripheral blood levels of the following markers: soluble interleukin (IL)-2 receptor-α (sIL2R; CellFree Human sIL2R, Endogen, Woburn, MA), a molecule cleaved from the surface of activated helper T-lymphocytes[25]; soluble CD30 (sCD30; Human sCD30 ELISA, Bender MedSystems, Vienna, Austria), which is a tumor necrosis factor receptor superfamily protein shed from activated B- and T-lymphocytes[26]; C-reactive protein (CRP; Virgo CRP 150, Hemagen Diagnostics, Columbia, MD), a stable marker of chronic inflammation and correlate of circulating IL-6 levels[27]; and neopterin (ELItest Neopterin EIA, BRAHMS Diagnostica GMBH, Berlin, Germany), which is induced by interferon-γ during innate (nonspecific) immune responses.[28] We also measured concentrations of total human immunoglobulin E (IgE), a marker of B-lymphocyte activation. Total IgE levels were determined by ELISA based on a modified Mouse IgE ELISA protocol (BD Biosciences Pharmingen, San Diego, CA), using anti-human IgE monoclonal antibodies (G7-18, G7-26, 2 μg/mL), and purified human IgE standard (31.2–500 ng/mL, Calbiochem, San Diego, CA); 1 ng/mL of the Calbiochem standard was comparable to 2 IU/mL of human IgE (NIBSC 75/502).

The detection limits of the immune marker assays were 0.25 μg/mL CRP, 6.4 U/mL sCD30, 40 pg/mL sIL2R, 2 nmol/L neopterin and 31 ng/mL total IgE. Samples with CRP and total IgE levels below the detection limit were assigned a value of half the corresponding assay's limit (*i.e.*, 0.13 μg/mL CRP or 15.5 ng/mL total IgE).

Statistical analysis

To characterize subjects' immune marker patterns, we classified levels of antibody to EBV nuclear antigen-2 (anti-EBNA2), EBV viral capsid antigen (anti-VCA), CRP, sIL2R, sCD30, neopterin and total IgE as greater than ("higher"), or less than or equal to ("lower"), the median levels observed among HTLV-I noncarriers from the same population. Because lower anti-EBNA1 titers are associated with diminished type 1 immunity,[22,29] we grouped anti-EBNA1 titers as greater than or equal to (higher), or less than (lower) the respective median titers. We dichotomized titers of antibody to EBV early antigen (anti-EA) as seropositive (≥1:20) or seronegative (<1:20). We computed the ratio of anti-EBNA1 to anti-EBNA2 titers; a ratio of 1.0 or lower (*i.e.*, "low EBNA1:EBNA2 ratio"), which occurs when the anti-EBNA1 titer is less than or equal to the anti-EBNA2 titer, is empirically associated with deficient control of EBV replication.[22,29]

All analyses adjusted for the matching factors. Regression models included age and sample collection year as continuous variables. Linear regression models and correlation computations utilized $\log_{10}$-transformations of the continuous immune and/or viral marker levels. To explore underlying population differences in immune status, we computed the geometric mean level of immune markers by population in HTLV-I non-carriers using mixed-effects linear regression analyses that accounted for the matching-related correlations in the data. We assessed population differences in the covariate-adjusted means by the *t*-test. We used the Mantel-Haenszel test, adjusted for age (<60 *vs.* 60+ years), gender and sample collection year (1987–1989 *vs.* 1990–1993), to examine population differences in the prevalence of anti-EA seropositivity and a low EBNA1:EBNA2 ratio. Odds ratios (OR) and Wald-type 95% confidence intervals (CI) were computed by logistic regression to examine the association of HTLV-I serostatus with a given immune marker category (*i.e.*, "higher" or "lower" levels), and (in carriers) to assess the immune markers' association